

Attention in Motion: Secure Platooning via Transformer-based Misbehavior Detection

Konstantinos Kalogiannis*^{id}, *Student Member, IEEE*, Ahmed Mohamed Hussain*^{id}, *Member, IEEE*, Hexu Li^{id},
and Panos Papadimitratos^{id}, *Fellow, IEEE*

Abstract—Vehicular platooning promises transformative improvements in transportation efficiency and safety through the coordination of multi-vehicle formations enabled by Vehicle-to-Everything (V2X) communication. However, the distributed nature of platoon coordination creates security vulnerabilities, allowing authenticated vehicles to inject falsified kinematic data, compromise operational stability, and pose a threat to passenger safety. Traditional misbehaviour detection approaches, which rely on plausibility checks and statistical methods, suffer from high False Positive (FP) rates and cannot capture the complex temporal dependencies inherent in multi-vehicle coordination dynamics. We present **Attention In Motion (AIMFORMER)**, a transformer-based framework specifically tailored for real-time misbehaviour detection in vehicular platoons with edge deployment capabilities. AIMFORMER leverages multi-head self-attention mechanisms to simultaneously capture intra-vehicle temporal dynamics and inter-vehicle spatial correlations. It incorporates global positional encoding with vehicle-specific temporal offsets to handle join/exit maneuvers. We propose a Precision-Focused Binary Cross-Entropy (PFBCE) loss function that penalizes FPs to meet the requirements of safety-critical vehicular systems. Extensive evaluation across 4 platoon controllers, multiple attack vectors, and diverse mobility scenarios demonstrates superior performance (≥ 0.93) compared to state-of-the-art baseline architectures. A comprehensive deployment analysis utilizing TensorFlow Lite (TFLite), Open Neural Network Exchange (ONNX), and TensorRT achieves sub-millisecond inference latency, making it suitable for real-time operation on resource-constrained edge platforms. Hence, validating AIMFORMER is viable for both in-vehicle and roadside infrastructure deployment.

Index Terms—Vehicular Platooning, Misbehavior Detection, Data-driven Approaches, Methods for Security and Privacy, Connected and Autonomous Vehicles, Vehicular Ad Hoc Networks.

I. INTRODUCTION

Internet of Vehicles (IoV) transforms modern transportation, with Vehicle-to-Vehicle (V2V) and Vehicle-to-Infrastructure (V2I) communication enabling cooperative driving applications [1]. Among the most promising representations of this vision is vehicle platooning. It enables multiple vehicles to travel in close formation with coordinated inter-vehicular spacing, yielding substantial improvements in traffic throughput, fuel efficiency, and safety [2], [3], [4], [5], [6]. Vehicular platoons operate through Cooperative Adaptive Cruise Control (CACC) systems that extend traditional Adaptive Cruise Control (ACC) capabilities by incorporating real-time

communication (Cooperative Awareness Message (CAM)) of kinematic data, including position, velocity, and acceleration via standardized protocols such as IEEE 802.11p or Cellular Vehicle-to-Everything (V2X) [1].

This fundamental reliance on continuous wireless information exchange, however, introduces critical security vulnerabilities that threaten both operational integrity and passenger safety [7], [5]. The distributed nature of platoon coordination creates an attack surface where malicious or compromised vehicles can inject falsified information to manipulate the behavior of other platoon members. Such attack consequences range from reduced stability to complete platoon destabilization and increased collision risks [8]. The effects can be further amplified when misbehavior originates from the platoon leader, given its key role in platooning. Unlike external adversaries, which can be thwarted by secure V2X protocols [1], [9], [10], [11], internal adversaries transmitting false kinematic data pose a significant challenge that requires real-time detection.

Traditional approaches to Misbehavior Detection Schemes (MDSs) in Vehicular Ad-hoc Network (VANET) have predominantly employed plausibility checks, statistical outlier detection, and rule-based behavioral analysis [12], [13]. While computationally efficient, these techniques suffer from several limitations: (i) high False Positive (FP) rates when encountering sophisticated attacks, (ii) inability to generalize across diverse platoon configurations and control policies, and (iii) inadequate modeling of complex temporal dependencies inherent in multi-vehicle coordination dynamics. The challenge is further compounded by the dynamic nature of platooning scenarios. Topology changes during vehicle *join* and *exit* maneuvers constitute prime moments for attack as they involve multiple cars, potentially in different lanes (e.g., during a join). Such attacks can be catastrophic not only to the platoon itself, but to other road users [14], [7], [15], with a two-fold challenge for misbehavior detection during maneuvering: FPs disrupt legitimate platoon operations, while False Negatives (FNs) enable successful attacks.

Several detection approaches emerged to address these limitations through diverse methodologies. Probabilistic methods employing Gaussian Mixture Model (GMM)-Hidden Markov Model (HMM) achieve 87% F1-score [7], specialized classifiers leverage Random Forest (RF) for rapid inference [16], [17], [18], and recurrent networks (Long Short-Term Memory (LSTM)/Gated Recurrent Unit (GRU)) demonstrate improved accuracy [19], [20]. Most closely related to our work, AttentionGuard [5] applies attention mechanisms to achieve 88-92% accuracy with 96-99% Area Under the Curve (AUC). However,

*Equally contributing authors. Konstantinos Kalogiannis, Ahmed Mohamed Hussain, and Panos Papadimitratos are with the Networked Systems Security (NSS) Group, KTH Royal Institute of Technology, Stockholm, Sweden. Email: {konkal, ahmhus, papadim}@kth.se. Hexu Li is with the Tech Validation – AI department at the Chief Technology Officer (CTO) Organization, Lenovo, Beijing, China. Email: lihx36@lenovo.com.

three essential constraints persist across these approaches: (i) inference latency incompatible with real-time requirements; (ii) reliance on manual feature engineering or position-specific architectures limiting cross-configuration generalization; (iii) sequential processing in recurrent networks. The latter prevents efficient parallel training while struggling to simultaneously capture both intra-vehicle temporal evolution and inter-vehicle spatial correlations, which are essential for detecting coordinated attacks during topology changes.

Transformer architectures [21] can address constraints (ii) and (iii) through self-attention mechanisms that enable parallel sequence processing while simultaneously modeling both intra-vehicle temporal dynamics and inter-vehicle spatial correlations. Thus, transformers can capture attack propagation patterns across platoon formations by jointly observing the evolution of individual vehicle behavior and cross-vehicle correlation structures. Such dual modeling capacity proves essential for distinguishing legitimate coordination dynamics from malicious manipulation, thereby minimizing FPs during legitimate maneuvers while maintaining robust detection of sophisticated, coordinated attacks.

Concurrently, the maturation of edge computing within vehicular networks enables deploying Machine Learning (ML) models closer to data sources, addressing the ultra-low latency requirements (typically under $100ms$) essential for safety-critical driving applications [22]. Edge Artificial Intelligence (AI) enables real-time inference on resource-constrained platforms while preserving privacy through localized processing and reducing communication overhead to centralized cloud infrastructure [23].

To address these combined challenges of real-time inference and sophisticated attack detection in platooning, this paper presents AIMFORMER, a transformer-based framework specifically designed for real-time misbehavior detection in vehicular platoons with edge deployment capabilities. Our approach leverages multi-head self-attention mechanisms to simultaneously capture intra-vehicle temporal dynamics and inter-vehicle coordination patterns, enabling comprehensive behavioral analysis across diverse attack vectors, platoon topologies, and operational scenarios.

Contribution. We summarize our contributions as follows:

- 1) We build on our prior work [5] and develop the first transformer-based misbehavior detection framework specifically designed for vehicular platooning environments, incorporating global positional encoding mechanisms that maintain temporal awareness across multi-vehicle sequences with asynchronous dynamics.
- 2) We propose a novel Precision-Focused Binary Cross-Entropy (PF BCE) loss function that addresses the precision-recall trade-off inherent in security-critical applications by introducing parameterized penalties for FP predictions while preserving attack detection capability through balanced positive class weighting.
- 3) We conduct an extensive comparative analysis across 4 different platoon controllers, various attack types (i.e., position, speed, acceleration falsification with constant, and gradual offsets), and mobility scenarios (e.g., join, exit, steady-state), demonstrating superior performance (≥ 0.93)

against baseline architectures including LSTM, BiLSTM, Convolutional Neural Network (CNN), CNN-LSTM, GRU, and Multi-Layer Perceptron (MLP).

- 4) We demonstrate the practical viability of edge deployment through comprehensive evaluation and analysis using popular frameworks (e.g., TensorFlow Lite (TFLite), Open Neural Network Exchange (ONNX), TensorRT), achieving sub-millisecond inference latencies suitable for real-time deployment on resource-constrained embedded platforms.

Paper Organization. Section II establishes technical preliminaries including IoV platooning architectures, edge AI, transformer encoder, and prevalent misbehavior categories. Section III formalizes our system and adversarial models. Section IV details the AIMFORMER architecture, feature engineering pipeline, training methodology, and deployment optimization strategies. Section V presents performance evaluation including ablation studies, baseline comparisons, and deployment analysis on edge hardware. Section VII surveys related work in vehicular misbehavior detection, transformer applications in security domains, and edge AI for Intelligent Transport Systems (ITS). Section VIII concludes with future research directions.

II. PRELIMINARIES

This section establishes the foundational concepts necessary for understanding the proposed framework: IoV platooning coordination, transformer encoder architecture, and the context of edge AI deployment.

A. Vehicular Platooning and V2V/V2I Communication

Vehicle platooning enables coordinated convoy formations through V2V and V2I communication, where CACC systems extend traditional ACC by exchanging real-time kinematic data (i.e., position, velocity, acceleration) via IEEE 802.11p or cellular V2X protocols.

Communication Topologies and Control Strategies: Platoon communication architectures operate through distinct topological configurations that determine information flow patterns. The predominant topologies include: *Predecessor-Following*, where vehicles receive information exclusively from their immediate predecessor, minimizing communication overhead but potentially suffering from error propagation; *Predecessor-Leader*, where vehicles maintain links with both predecessor and platoon leader, enhancing string stability through dual information sources; and *Bidirectional Communication*, where vehicles exchange information with both preceding and following vehicles, facilitating enhanced situational awareness and disturbance rejection capabilities.

Platoon coordination employs two primary spacing policies: *Constant Time Headway (CTH)* maintains time-based following distances that scale with vehicle speed, enhancing stability at higher velocities while reducing road utilization efficiency; *Constant Vehicle Spacing (CVS)* enforces fixed physical distances regardless of speed, maximizing road capacity but requiring precise control mechanisms during dynamic maneuvers.

Several control strategies implement these policies: PATH (CVS with Predecessor-Leader topology), Ploeg (CTH with Predecessor-Following topology), Consensus (hybrid policy with multi-source information), and Flatbed (CVS with leader and predecessor speed information). These different information flows and controller policies lead to varied vulnerability susceptibility and platoon reactions [8], [7], [24].

B. Transformer Encoder Architecture

The Transformer encoder utilizes self-attention mechanisms for parallel sequence processing, capturing long-range dependencies without the computational limitations inherent in Recurrent Neural Networks (RNNs).

Self-Attention Mechanism. The self-attention mechanism operates by transforming input sequences into three fundamental representations: queries (Q), keys (K), and values (V). For an input sequence x_1, x_2, \dots, x_n where each $x_i \in \mathbb{R}^d$, the scaled dot-product attention computes:

$$\text{Attention}(Q, K, V) = \text{softmax}\left(\frac{QK^T}{\sqrt{d}}\right)V \quad (1)$$

This formulation enables each sequence position to attend to all other positions simultaneously, creating a comprehensive representational model that captures complex temporal dependencies essential for time-series analysis tasks.

Multi-Head Attention and Positional Encoding. Multi-head attention extends the self-attention mechanism by computing multiple attention operations in parallel across different representational subspaces. This parallel processing enables the model to capture diverse types of dependencies simultaneously, with different attention heads specializing in distinct relational patterns within the data. The multi-head attention mechanism is defined as:

$$\text{MultiHead}(Q, K, V) = \text{Concat}(\text{head}_1, \dots, \text{head}_h)W^O \quad (2)$$

where each attention head operates in a lower-dimensional subspace, allowing the model to focus on different aspects of the input sequence concurrently. Since the attention mechanism lacks inherent sequential ordering information, positional encoding provides the model with explicit positional awareness. The Transformer employs sinusoidal positional encodings that are added directly to input embeddings, enabling the model to distinguish between different temporal positions while maintaining the ability to generalize to sequences of varying lengths.

C. Edge AI Deployment Context

Edge AI enables ML model execution on devices proximate to data sources, addressing latency, bandwidth, and privacy constraints inherent in cloud-centric approaches [25], [26]. For safety-critical vehicular applications requiring sub-100ms response times, edge deployment facilitates real-time misbehavior detection while preserving the benefits of localized processing. Recent embedded implementations demonstrate compact Deep Neural Network (DNN) architectures achieving high accuracy on resource-constrained hardware [27], [28],

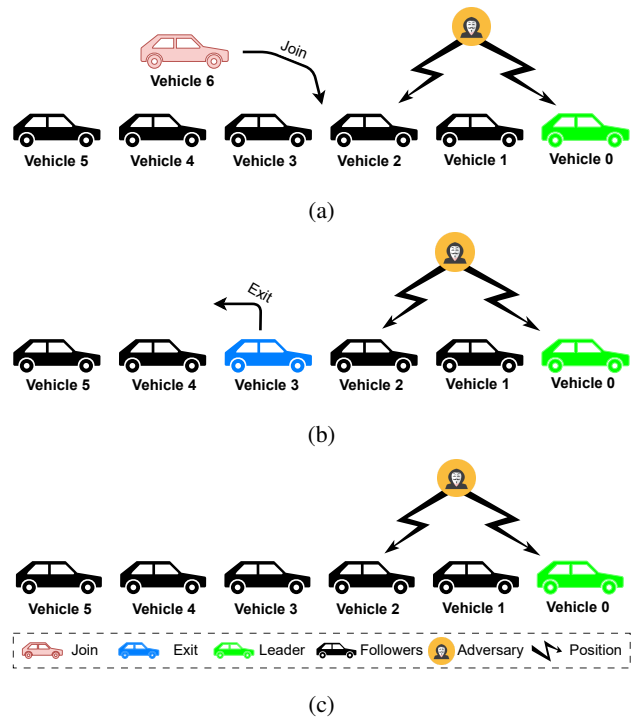


Fig. 1: Attacks during platoon topology changes. (a) *Join* maneuver: a new vehicle (Vehicle 6) attempts to merge into the platoon while an adversary forges/perturbs kinematic information. (b) *Exit* maneuver: a member (Vehicle 3) leaves the platoon while the adversary initiates the message manipulation. (c) *Steady-State*: the attacker performs a falsification attack on the platoon during normal cruising.

[29], making distributed security frameworks feasible for vehicular platoons. Within the platooning context specifically, edge AI enables distributed misbehavior detection, real-time trust management, and adaptive coordination that leverage local processing capabilities while minimizing communication overhead to centralized infrastructure.

III. SYSTEM AND ADVERSARIAL MODEL

A. System Model

We consider vehicles implementing V2X protocol stacks [30] equipped with valid Vehicular Communication (VC) cryptographic credentials obtained through legitimate vehicle registration, allowing them to participate in V2X communications and platooning operations [31], [10], [11], [32]. Successful misbehavior detection can trigger the credential revocation mechanisms, preventing future malicious participation in platoon operations. Platoons operate under a designated leader who coordinates vehicle enrollment and departure occurring through individual vehicle join/exit maneuvers or platoon merging operations. Upon admission, joining vehicles position themselves at leader-designated locations, and the updated configuration is broadcast to all members. Our system model assumes a string-stable platoon of vehicles traveling on a highway segment, allowing for join/exit maneuvers at any position based on vehicle capabilities and destination compatibility.

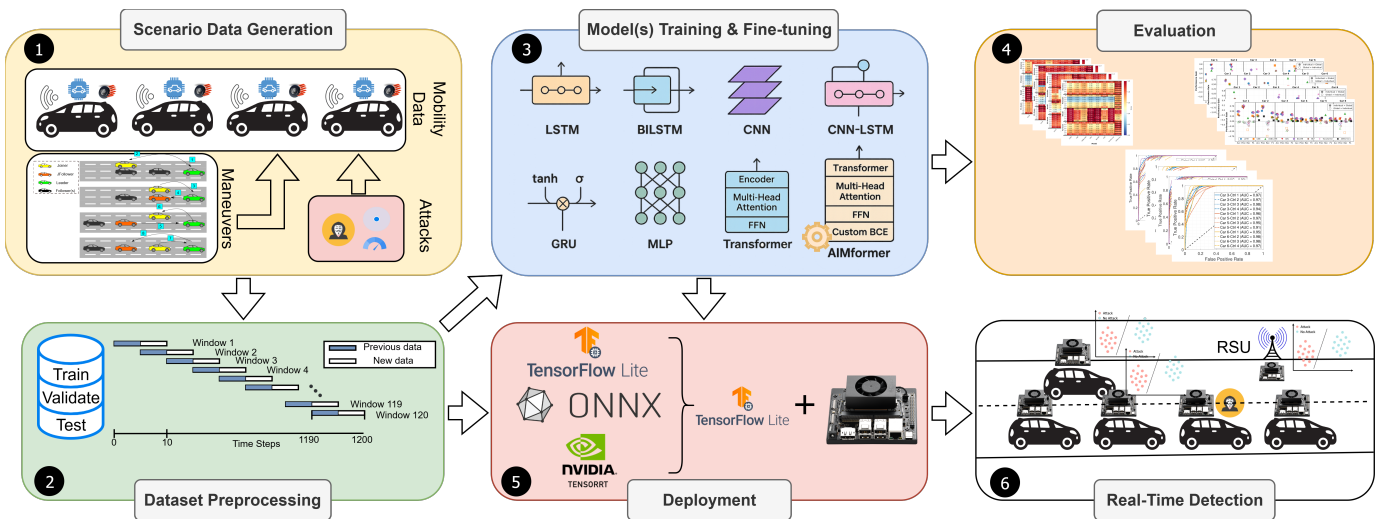


Fig. 2: Pipeline for edge AI-based V2X attack detection: **1** Scenario data generation with mobility traces, maneuvers, and attacks; **2** dataset preprocessing and temporal windowing into train/validation/test splits; **3** model training with LSTM, BiLSTM, CNN, CNN-LSTM, GRU, MLP, and Transformer/AIMFORMER (custom Binary Cross-Entropy (BCE)); **4** offline evaluation (confusion matrices, metrics, ROC); **5** deployment via TFLite, ONNX, and TensorRT to embedded hardware; and **6** real-time detection on vehicles/RSUs. Arrows indicate the end-to-end workflow.

B. Adversarial Models

We consider internal adversaries equipped with valid cryptographic credentials, obtained through legitimate vehicle registration. Following the general adversary model for secure and privacy-preserving VC systems [1], [33] and vehicular platooning assumptions [3], [8], [34], [35], these authenticated attackers can participate in V2X communications and transmit messages accepted as legitimate by other platoon members. However, internal adversaries cannot extract private keys that are stored in Hardware Security Modules (HSMs) [1], provisioned during the vehicle registration [10]. Adversarial behavior stems from direct vehicle control, or malware intercepting internal data streams (e.g., Controller Area Network (CAN) bus messages, sensor outputs) before V2X transmission.

Internal adversaries mount falsification attacks by manipulating kinematic data in transmitted CAMs. Specifically, we consider three data falsification attacks executed by rational adversaries who maximize attack effectiveness while minimizing self-harm [7]. First, attackers can broadcast incorrect positional coordinates, misleading neighboring vehicles about their actual location. This attack type particularly affects controllers that rely on absolute positioning information for distance calculations and coordination decisions. Second, malicious vehicles can report incorrect velocity values, causing platoon followers to make inappropriate acceleration decisions. The severity of impact varies based on control strategy, with CVS-based controllers showing greater vulnerability to speed-based attacks. Finally, attackers can transmit false acceleration data. This attack type can cause immediate and severe destabilization effects across diverse controller implementations.

Attack Windows. The platoon topology reconfiguration events represent critical vulnerability windows: during join and exit maneuvers, platoons experience temporary instability characterized by modified communication topologies, redis-

tributed control responsibilities, and heightened requirements for accurate state information exchange. Adversaries exploit these transitional phases to amplify attack effectiveness and maximize disruption potential.

Attack Scenarios. Fig. 1 illustrates three attack scenarios: (a) *Join Maneuver* where Vehicle 6 integrates while the adversary broadcasts falsified kinematic data, targeting the admission and spacing phase to create unsafe gaps or collision risks; (b) *Exit Maneuver* where the adversary manipulates CAMs during Vehicle 3's departure, exploiting the critical period when remaining vehicles reestablish predecessor-follower relationships; and (c) *Steady-State* where the adversary performs data falsification during normal cruising operations without topology changes. For each attack scenario, we consider both an attacker leading the platoon and an attacker traveling just ahead of the maneuvering position. This setup ensures both maximal attack reach (leader attacker) and amplified attack impact (vehicle 2 attacker) by potentially causing collisions in both lanes (as the maneuvering vehicle changes lanes) [7].

We examine 9 distinct attack types spanning three manipulation strategies [7]: *Constant Offset Attacks* introducing fixed biases to position, velocity, or acceleration; *Gradual Offset Attacks* applying time-varying drift to kinematic parameters; and *Combined Physics-Consistent Attacks* simultaneously falsifying multiple state variables while maintaining kinematic feasibility to evade simple plausibility checks.

IV. PROPOSED FRAMEWORK AND IMPLEMENTATION

A. Proposed Framework

Fig. 2 presents our end-to-end attack detection pipeline from data generation to deployment. In step **1**, we generate scenario data incorporating diverse mobility patterns (middle-join, middle-exit, normal traveling) across different platoon formations with attackers in various positions (described in III-B).

The mobility features are sourced from ego-vehicle sensors, each with its own sensor errors (as described in [7]), which capture the resulting mobility effects after controller actuation. The deployed MDS learns to distinguish misbehavior from nominal mobility based on these patterns. Step ② preprocesses the mobility data into normalized train/validation/test sets, segmenting them into windows of ten messages (1 second) with $100m.s$ step size, enabling inference after each disseminated CAM. Each timestep receives a label (attack/no attack) and mask (Eq. 11).

Step ③ involves training baseline architectures (LSTM, Bidirectional LSTM (BiLSTM), CNN, CNN-LSTM, GRU, MLP, Transformer) and our AIMFORMER solution, creating both global models (deployable in Roadside Units (RSUs)) and individual vehicle-specific models (Section IV-C). Step ④ evaluates all models on the unseen test set, applying iterative refinement (Section V). Step ⑤ converts and quantizes models via TFLite, ONNX, and TensorRT for resource-constrained deployment, evaluating inference time and memory footprint (Section V-C). Finally, step ⑥ analyzes individual versus global model performance across platoon positions (Section V-B).

TABLE I: Mathematical notation for the Transformer-encoder.

Symbol	Description
Model Parameters	
\mathbf{W}_{embed}	Input embedding weight matrix
\mathbf{b}_{embed}	Input embedding bias vector
\mathbf{W}_i^Q	Query projection matrix for head i
\mathbf{W}_i^K	Key projection matrix for head i
\mathbf{W}_i^V	Value projection matrix for head i
\mathbf{W}_i^O	Multi-head output projection matrix
\mathbf{W}_1	First feed-forward weight matrix
\mathbf{W}_2	Second feed-forward weight matrix
\mathbf{b}_1	First feed-forward bias vector
\mathbf{b}_2	Second feed-forward bias vector
\mathbf{W}_{out}	Output projection weight matrix
\mathbf{b}_{out}	Output projection bias
Hidden States and Intermediate Tensors	
$\mathbf{H}^{(0)}$	Initial embedded representations
$\tilde{\mathbf{H}}^{(\ell)}$	Hidden states after layer ℓ
$\mathbf{A}^{(\ell)}$	Attention output at layer ℓ
$\mathbf{H}_1^{(\ell)}$	Intermediate hidden states at layer ℓ
$\mathbf{F}^{(\ell)}$	Feed-forward output at layer ℓ
\mathbf{O}_{flat}	Flattened output before reshaping
Attention Mechanism	
\mathbf{Q}	Query matrix
\mathbf{K}	Key matrix
\mathbf{V}	Value matrix
$head_i$	Output of attention head i
\mathbf{M}	Combined attention mask
\mathbf{M}_{pad}	Padding mask
\mathbf{M}_{causal}	Causal mask

B. Model Design

Model Architecture. We present a Transformer-based architecture for single- or multi-vehicle binary classification. Given input $\mathbf{X} \in \mathbb{R}^{B \times V \times T \times F}$ (batch size B , vehicles V , sequence length T , features F), the model produces binary predictions $\hat{\mathbf{Y}} \in \mathbb{R}^{B \times V \times T}$ for each timestep. Global positional

encoding with vehicle-specific temporal offsets aligns the vehicles individual time windows to the overall vehicle trip:

$$\mathbf{P}_{v,t} = PE(g_{v,t}) \quad (3)$$

$$g_{v,t} = t + \text{offset}_v \quad (4)$$

where $g_{v,t}$ represents the global time position for vehicle v at local timestep t . Input processing reshapes and embeds multi-vehicle data for parallel computation:

$$\mathbf{X}_{flat} = \text{reshape}(\mathbf{X}, [B \cdot V, T, F]) \quad (5)$$

$$\mathbf{H}^{(0)} = \mathbf{X}_{flat} \mathbf{W}_{embed} + \mathbf{b}_{embed} \quad (6)$$

$$\tilde{\mathbf{H}}^{(0)} = \mathbf{H}^{(0)} + \mathbf{P} \quad (7)$$

where $\mathbf{W}_{embed} \in \mathbb{R}^{F \times d_{model}}$, $\mathbf{b}_{embed} \in \mathbb{R}^{d_{model}}$ are embedding parameters, and $\mathbf{P} \in \mathbb{R}^{B \cdot V \times T \times d_{model}}$ contains positional encodings. Multi-head self-attention is formulated as:

$$\text{MultiHead}(\mathbf{Q}, \mathbf{K}, \mathbf{V}) = \text{Concat}(\text{head}_1, \dots, \text{head}_h) \mathbf{W}^O \quad (8)$$

$$\text{head}_i = \text{Attention}(\mathbf{Q} \mathbf{W}_i^Q, \mathbf{K} \mathbf{W}_i^K, \mathbf{V} \mathbf{W}_i^V) \quad (9)$$

$$\text{Attention}(\mathbf{Q}, \mathbf{K}, \mathbf{V}) = \text{softmax} \left(\frac{\mathbf{Q} \mathbf{K}^T}{\sqrt{d_k}} + \mathbf{M} \right) \mathbf{V} \quad (10)$$

where $\mathbf{W}_i^Q, \mathbf{W}_i^K, \mathbf{W}_i^V \in \mathbb{R}^{d_{model} \times d_k}$ are projection matrices, $d_k = d_{model}/h$, and \mathbf{M} is the attention mask (Table I). The masking strategy combines padding and causal constraints for variable-length sequences with asynchronous entry/exit times:

$$\mathbf{M}_{pad}[i, j] = \begin{cases} 0, & \text{if position } j \text{ is valid for sequence } i \\ -\infty, & \text{if position } j \text{ is padded for sequence } i \end{cases} \quad (11)$$

$$\mathbf{M}_{causal}[i, j] = \begin{cases} 0, & \text{if } j \leq i \\ -\infty, & \text{if } j > i \end{cases} \quad (12)$$

$$\mathbf{M} = \mathbf{M}_{pad} \quad (13)$$

Each encoder block $\ell \in \{1, 2, \dots, L\}$ applies standard Transformer operations with residual connections and layer normalization:

$$\mathbf{A}^{(\ell)} = \text{MultiHead}(\tilde{\mathbf{H}}^{(\ell-1)}, \tilde{\mathbf{H}}^{(\ell-1)}, \tilde{\mathbf{H}}^{(\ell-1)}) \quad (14)$$

$$\mathbf{H}_1^{(\ell)} = \text{LayerNorm}(\tilde{\mathbf{H}}^{(\ell-1)} + \text{Dropout}(\mathbf{A}^{(\ell)})) \quad (15)$$

$$\mathbf{F}^{(\ell)} = \text{FFN}(\mathbf{H}_1^{(\ell)}) \quad (16)$$

$$\tilde{\mathbf{H}}^{(\ell)} = \text{LayerNorm}(\mathbf{H}_1^{(\ell)} + \text{Dropout}(\mathbf{F}^{(\ell)})) \quad (17)$$

where the feed-forward network is:

$$\text{FFN}(\mathbf{x}) = \text{ReLU}(\mathbf{x} \mathbf{W}_1 + \mathbf{b}_1) \mathbf{W}_2 + \mathbf{b}_2 \quad (18)$$

with $\mathbf{W}_1 \in \mathbb{R}^{d_{model} \times d_{ff}}$, $\mathbf{W}_2 \in \mathbb{R}^{d_{ff} \times d_{model}}$, and typically $d_{ff} = 4 \cdot d_{model}$. Final output projection recovers the multi-vehicle structure:

$$\mathbf{O}_{flat} = \tilde{\mathbf{H}}^{(L)} \mathbf{W}_{out} + \mathbf{b}_{out} \quad (19)$$

$$\hat{\mathbf{Y}} = \text{reshape}(\mathbf{O}_{flat}, [B, V, T]) \quad (20)$$

where $\mathbf{W}_{out} \in \mathbb{R}^{d_{model} \times 1}$ and $\mathbf{b}_{out} \in \mathbb{R}$ are binary classification parameters.

This architecture captures intra-vehicle temporal dependencies through self-attention operating independently over each vehicle's time series, with global positional encoding providing trajectory-phase awareness. The vehicle-independent processing enables flexible deployment as either global (multi-vehicle) or individual (single-vehicle) models, without requiring architectural modifications.

TABLE II: Mathematical notation for Precision-Focused BCE Loss function.

Symbol	Description
Input Variables	
$y_{i,j}$	Ground truth binary label for vehicle i at time step j
$\hat{y}_{i,j}$	Predicted logit for vehicle i at time step j
$m_{i,j}$	Binary loss mask for vehicle i at time step j
Sets and Derived Variables	
\mathcal{M}	Set of valid vehicle-time observations, $\{(i,j) : m_{i,j} = 1\}$
$ \mathcal{M} $	Number of valid vehicle-time observations
$\ell_{i,j}$	Standard BCE loss for vehicle i at time step j
$w_{FP}^{(i,j)}$	FP penalty weight for vehicle i at time step j
$w_{pos}^{(i,j)}$	Positive class weight for vehicle i at time step j
Hyperparameters	
λ_{FP}	FP penalty weight
λ_{pos}	Positive class weight
τ	FP threshold
ϵ	Numerical stability constant
Functions	
$\sigma(\cdot)$	Sigmoid activation function, $\sigma(z) = \frac{1}{1+e^{-z}}$
$\mathcal{L}_{PFBCE}(\cdot)$	Precision-focused BCE loss

Loss Function. We propose PFBCE to enhance precision by explicitly penalizing FPs while maintaining balanced treatment of positive samples, enabling detection of attack-influenced behavior that mimics nominal mobility [5]:

$$\mathcal{L}_{PFBCE}(\mathbf{y}, \hat{\mathbf{y}}) = \frac{1}{|\mathcal{M}|} \sum_{i,j \in \mathcal{M}} \ell_{i,j} \cdot w_{FP}^{(i,j)} \cdot w_{pos}^{(i,j)} \cdot m_{i,j} \quad (21)$$

where:

$$\ell_{i,j} = -y_{i,j} \log(\sigma(\hat{y}_{i,j})) - (1 - y_{i,j}) \log(1 - \sigma(\hat{y}_{i,j})) \quad (22)$$

$$w_{FP}^{(i,j)} = \begin{cases} \lambda_{FP}, & \text{if } y_{i,j} = 0 \text{ and } \sigma(\hat{y}_{i,j}) > \tau \\ 1, & \text{otherwise} \end{cases} \quad (23)$$

$$w_{pos}^{(i,j)} = \begin{cases} \lambda_{pos}, & \text{if } y_{i,j} = 1 \\ 1, & \text{if } y_{i,j} = 0 \end{cases} \quad (24)$$

$$|\mathcal{M}| = \sum_{i,j} m_{i,j} + \epsilon \quad (25)$$

The FP penalty $w_{FP}^{(i,j)}$ penalizes positive predictions ($\sigma(\hat{y}_{i,j}) > \tau$) on benign samples, encouraging conservative classification. The positive class weight $w_{pos}^{(i,j)}$ addresses class imbalance through moderate upweighting (λ_{pos}), maintaining sensitivity while benefiting from precision enhancement. The mask $m_{i,j}$ excludes invalid data (different entry/exit times or inapplicable scenarios), with normalization by $|\mathcal{M}|$ ensuring consistent loss magnitude (Table II).

Why PFBCE Over Focal Loss. Focal Loss emphasizes hard examples through $(1-p_t)^\gamma$, but treats all difficult samples uniformly regardless of error type, preventing direct control of the precision-recall trade-off. PFBCE instead provides explicit and interpretable error asymmetry: the FP penalty w_{FP} selectively suppresses confident incorrect positives to improve precision, while the positive-class weight w_{pos} independently handles class imbalance to tune recall. This decoupled design enables precise control over precision-recall behavior that Focal Loss cannot provide.

C. Training and Tuning

Model Training. We design two modeling approaches: *global* models trained on all platoon vehicles' data to learn whole-platoon mobility patterns, and *individual* models trained per-vehicle for position-specific local classification.

Model Tuning. We performed hyperparameter tuning using Keras Tuner's Hyperband algorithm [36], which efficiently balances exploration and computational cost by early termination of poor trials. Following Han et al. [37], we tuned the following parameters: hidden dimensions, attention heads, encoder blocks, dropout rate, and learning rate. Batch size (128) balances training time and generalization [38]. Table III summarizes tuned parameters for both model types. The global model preferred more encoder blocks (4 vs. 2) with identical hidden dimensions and attention heads, reflecting that simpler models generalize better on limited per-vehicle data.

TABLE III: Hyperparameter Tuning for Both Model Types

Hyperparameter	Search Space	Value	
		Global	Individual
Hidden Dimension	{128, 256, 320, 384}	128	128
Number of Attention Heads	{2, 4, 6}	2	2
Number of Encoder Blocks	{2, 3, 4}	4	2
Dropout Rate	[0.1, 0.2]	0.1	0.1
Learning Rate	$[10^{-5}, 10^{-3}]$ (log sampling)	1×10^{-4}	1×10^{-4}

Loss Tuning. Based on Eq. 21, we tuned weights and thresholds to balance FPs and FNs. Reducing positive weight (λ_{pos}) improved learning, while increasing attack threshold ($0.5 \rightarrow 0.6$) improved classification metrics (Section V-A). We investigated the F1-score-based loss; however, PFBCE provided superior balance without sacrificing precision (Table IV).

TABLE IV: Loss Function Tuning

Parameters	Search Space	Value
Loss Function	{PFBCE, BCE, F1BCE}	PFBCE
λ_{FP}	{1.6, 1.7, 1.8, 1.85, 1.9, 2}	1.7
λ_{pos}	{0.5, 0.7, 0.75, 0.9, 1}	0.6
τ	{0.5, 0.6, 0.7}	0.6

All models were trained, tuned, and evaluated using the attack data ratios in Table V. The variations reflect controller susceptibility to specific attacks, with vehicles downstream of the attacker (position 2) experiencing higher attack exposure.

TABLE V: Attack Ratio [%] shown as Train/Val/Test

Vehicle	Controller 1			Controller 2			Controller 3			Controller 4		
	Train	Val	Test									
Global	12.66	12.94	12.72	11.14	12.26	9.63	17.36	17.69	15.44	20.22	21.14	19.81
Car 1	11.02	11.09	11.26	5.00	4.94	5.04	15.44	16.57	12.70	14.40	15.72	14.59
Car 2	11.22	11.38	11.26	6.35	6.94	5.04	15.78	16.92	13.01	14.43	15.74	14.59
Car 3	13.63	14.88	13.06	13.61	15.47	11.60	17.67	17.43	16.46	22.21	24.48	21.10
Car 4	18.53	18.77	18.94	18.17	19.88	15.70	25.62	25.32	23.10	34.77	35.13	34.32
Car 5	18.69	18.79	18.94	19.20	21.55	15.80	25.39	25.13	22.91	33.83	34.09	33.54
Car 6	20.95	20.79	20.91	24.27	26.07	23.01	29.80	31.70	28.98	25.30	26.25	22.09

V. PERFORMANCE EVALUATION

A. Evaluation Metrics

Our testing process encompasses three evaluation types: (i) global model on whole-platoon data (*General Input*), (ii) global model on individual vehicle data (*Vehicle-specific Input*), and (iii) individual models on their own vehicle data. This investigation reveals trade-offs between locally- and edge-deployed models in platooning environments.

We utilize binary classification metrics (i.e., *recall*, *precision*, F_1 *score*, *accuracy*). With padding and masking, the underlying True Positive (TP), FP, FN, True Negative (TN) are:

$$\begin{aligned}
 TP &= \sum_i m_{i,j} \mathbf{1}(y_i = 1 \wedge \hat{y}_i = 1), \\
 FP &= \sum_i m_{i,j} \mathbf{1}(y_i = 0 \wedge \hat{y}_i = 1), \\
 FN &= \sum_i m_{i,j} \mathbf{1}(y_i = 1 \wedge \hat{y}_i = 0), \\
 TN &= \sum_i m_{i,j} \mathbf{1}(y_i = 0 \wedge \hat{y}_i = 0).
 \end{aligned} \tag{26}$$

For model comparison, we use Receiver Operating Characteristic (ROC) (displaying True Positive Rate (TPR) over False Positive Rate (FPR)) and AUC. We define Performance Gain (PG) for vehicle v and metric m as:

$$PG_{v,m} = \text{Individual}_{v,m} - \text{Global}_{v,m}, \tag{27}$$

where $\text{Individual}_{v,m}$ and $\text{Global}_{v,m}$ represent individual and global model performance, respectively.

B. AIMFORMER vs. Baseline Architectures

To showcase AIMFORMER superiority, we implemented seven baseline DNN architectures commonly used for time-series and misbehavior detection in IoVs [39], [40]. Table VI summarizes all models, including layers, parameters, and model sizes. BiLSTM has the highest parameter count due to bidirectional processing, while unidirectional LSTM reduces parameters by 62-63%. GRU uses bidirectional processing with simpler gating ($\approx 24\%$ fewer parameters). Feedforward architectures (CNN, MLP) have considerably lower parameter counts. The hybrid CNN-LSTM achieves efficiency through convolutional feature extraction before recurrent processing.

The baseline Transformer achieves the smallest sizes (1.6 MB global, 0.4 MB individual; 79% parameter reduction for individual models).

AIMFORMER's distinguishing features include: positional encoding with temporal offset awareness (Eqs. 3 and 4), three dropout operations per block (0.1 rate), two normalizations per block, and the custom PFBCE loss (Eq. 21) that penalizes FPs while weighting positive samples (Eq. 24). However, this complexity is reflected in the number of parameters (highest) and footprint (12 MB global, 6.2 MB individual). Nonetheless, quantization achieves significant size reduction (Table VII), facilitating edge deployment.

Fig. 3 presents classification metrics for all architectures across vehicle positions (C1-C6) and global input (G), for the global model, with black borders marking best performers. Across all controllers, AIMFORMER consistently outperforms baselines. For Controller 1 (Fig. 3a), most models achieve $> 80\%$ accuracy but struggle with precision-recall balance due to class imbalance; AIMFORMER's global input outperforms individual inputs for positions C4-C6. Controller 2 (Fig. 3b) shows CNN-LSTM achieving the highest precision but the lowest recall (overly conservative); AIMFORMER demonstrates superior F1-scores across all positions. For Controller 3 (Fig. 3c), GRU achieves low FPs but high FNs; AIMFORMER maintains high recall (critical for safety) while effectively detecting attacks in challenging positions C3-C5. Controller 4 (Fig. 3d) validates AIMFORMER's balanced precision-recall trade-off, yielding substantially higher F1-scores across all cars.

Fig. 4 illustrates the PG (Eq. 27) comparing individual vs. global models (filled icons: individual superior; empty: global superior). Upstream vehicles (C1-C2) consistently benefit from individual models, while C6 exhibits controller-dependent behavior. Vehicles C3 to C5 show architecture-dependent trends that favor individual models. Notably, AIMFORMER exhibits performance parity between deployment approaches, with one exception (Controller 1, C6: global model superior by $\approx 8\%$ F1). This performance consistency, coupled with global model results (highlighted in Fig. 3, row G), demonstrates AIMFORMER's ability to learn position-dependent patterns through the entire platoon input, making it optimal for both vehicle-local and RSU-based deployment in real-world V2X scenarios. Moreover, our vehicle-independent processing approach further enables scalability to larger platoons. Since self-attention operates independently over each vehicle's time series, the global model's generalization across C0 to C6 directly extends to additional vehicles, resulting in larger platoon sizes, without requiring architectural modifications.

C. AIMFORMER Deployment

We evaluate AIMFORMER on the Jetson Orin Nano Super Developer Kit, employing model quantization [28] across three optimization frameworks: (i) TFLite (direct TensorFlow transformation), (ii) ONNX (CPU and CUDA configurations on Jetson Orin Nano Super Developer Kit), and (iii) TensorRT (hardware-optimized). Both individual and global models are optimized using *float16* and *int8* quantization.

TABLE VI: Detailed architecture specifications and complexity of baseline models.

Model	Layers	Dense Layers	Dropout	Special Features	Parameters		Model Size [MB]	
					Global	Individual	Global	Individual
LSTM	3xLSTM(128)	128, 64, 1	0.3, 0.2	Unidirectional	379137	357633	4.5	4.2
BiLSTM	3xBiLSTM(128)	128, 64, 1	0.3, 0.2	Bidirectional	1011969	968961	12	12
GRU	3xBiGRU(128)	128, 64, 1	0.3, 0.2	Bidirectional	771585	739329	9	8.6
CNN-LSTM	2xConv1D + 2xBiLSTM	128, 64, 1	0.3, 0.2	BatchNorm, MaxPool	487297	479233	5.7	5.6
Transformer	MHA(8 heads, 64)+FFN	128, 64, 1	0.1, 0.3, 0.2	Self-attention, LayerNorm	129575	27179	1.6	0.417
CNN	3xConv1D + GlobalMaxPool	256, 128, 1	0.4, 0.3	BatchNorm, MaxPool	233345	225281	2.8	2.7
MLP	Flatten + 5xDense	512, 256, 128, 64, 1	0.4, 0.3, 0.2, 0.1	BatchNorm	427009	211969	5	2.5
AIMFORMER (Ours)	MHA (2 heads, 128) + FFN	128, 4x or 2x (512, 128), 1	0.1 (3x per block)	Positional Encoding, Self-attention, 2xLayerNorm, Residual, Custom Loss	1057921	529537	12.3	6.2

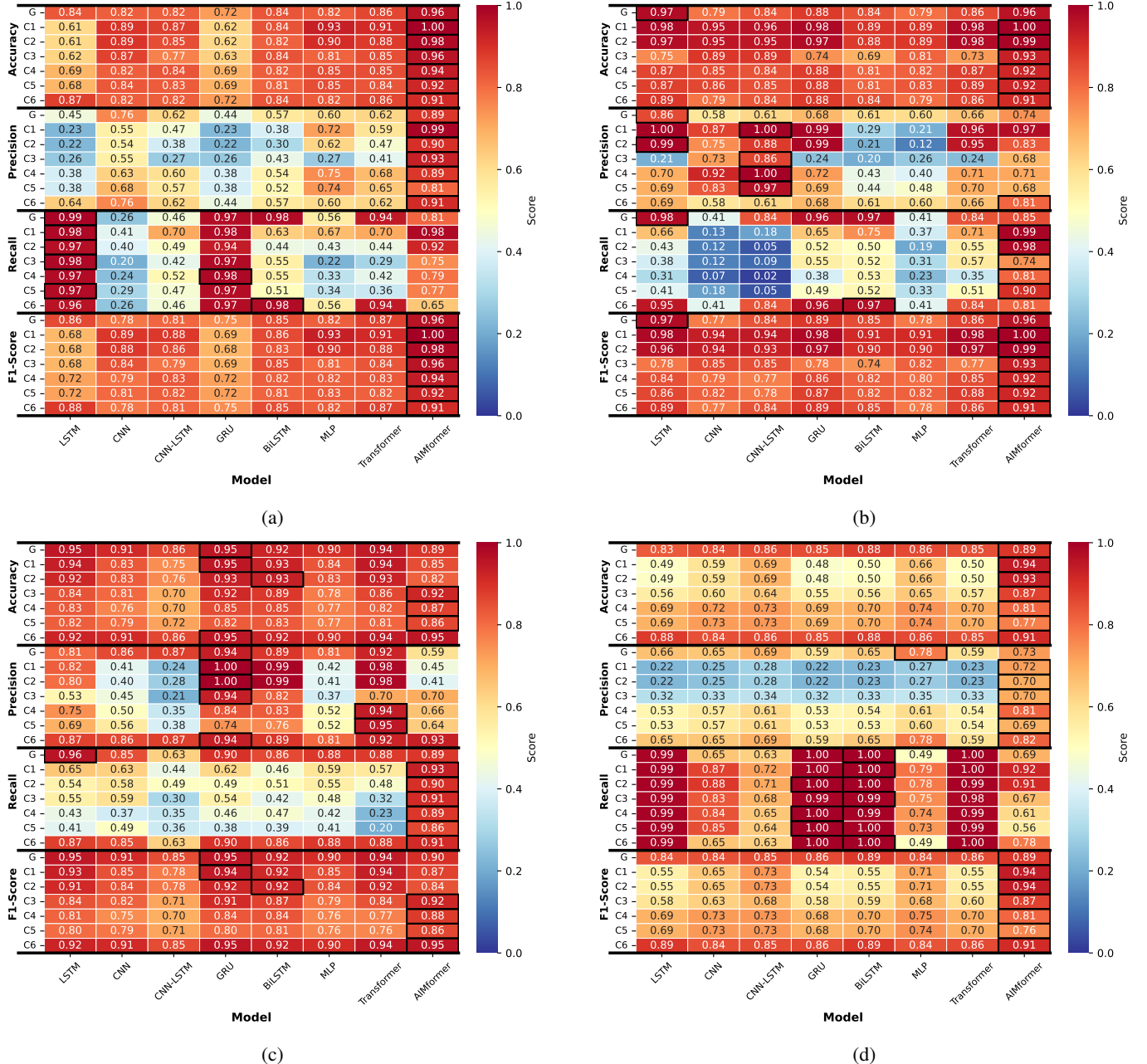
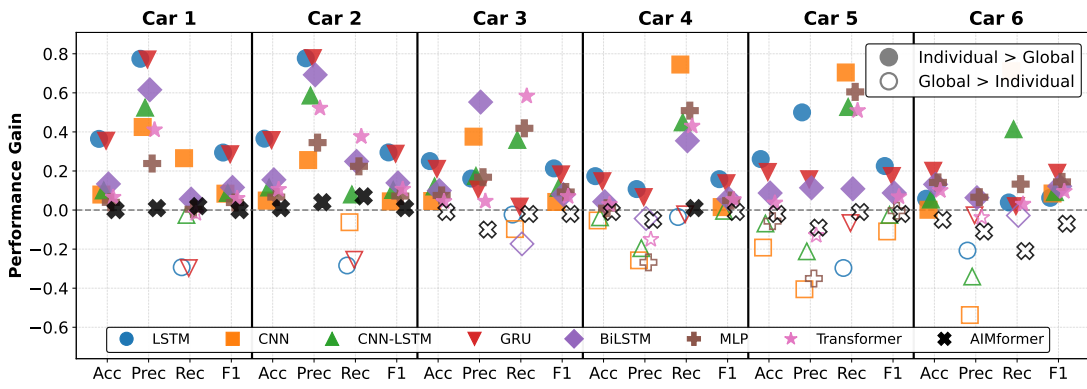


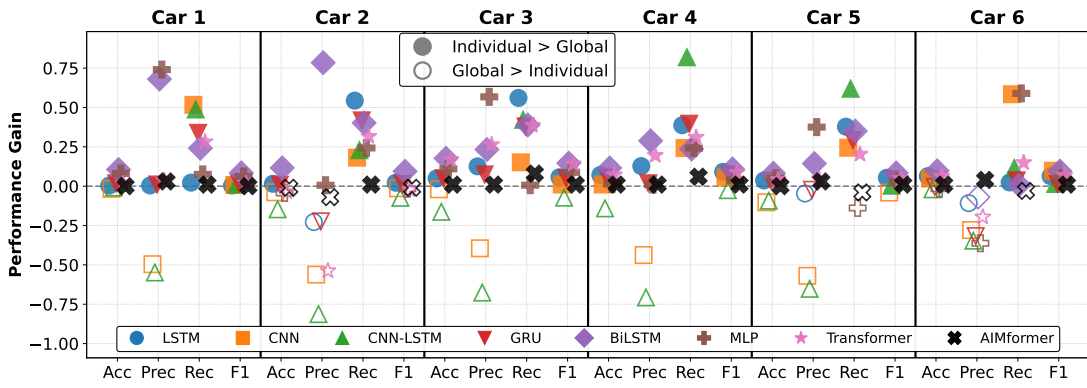
Fig. 3: Controllers comparison for general and vehicle-specific input. (a) Controller 1, (b) Controller 2, (c) Controller 3, (d) Controller 4.

Fig.5 presents average inference times for 1000 runs across all controllers. TFLite achieves fastest inference (0.13ms for individual models). Inference time differences across controllers are minimal due to similar model inputs and sizes

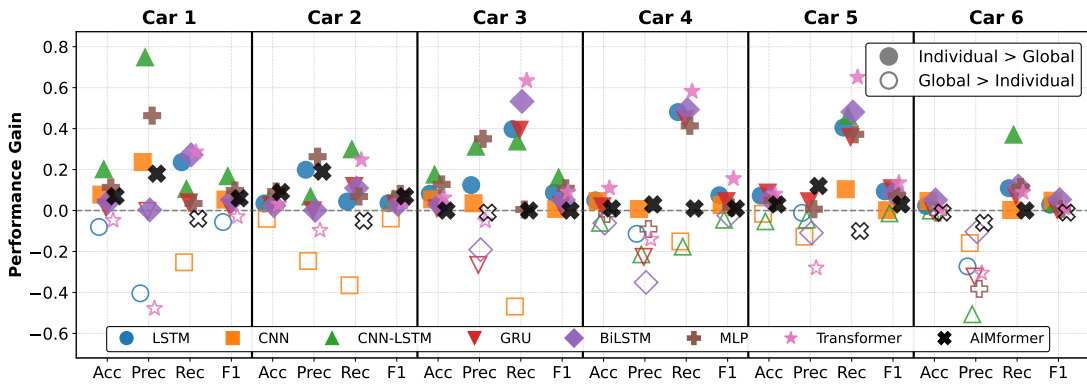
(Table VI). Individual models infer 50-90% faster than global models due to smaller size and input dimensionality. Float quantization is $\approx 2.5\times$ slower than integer quantization due to type-casting overhead, indicating integer quantization pref-



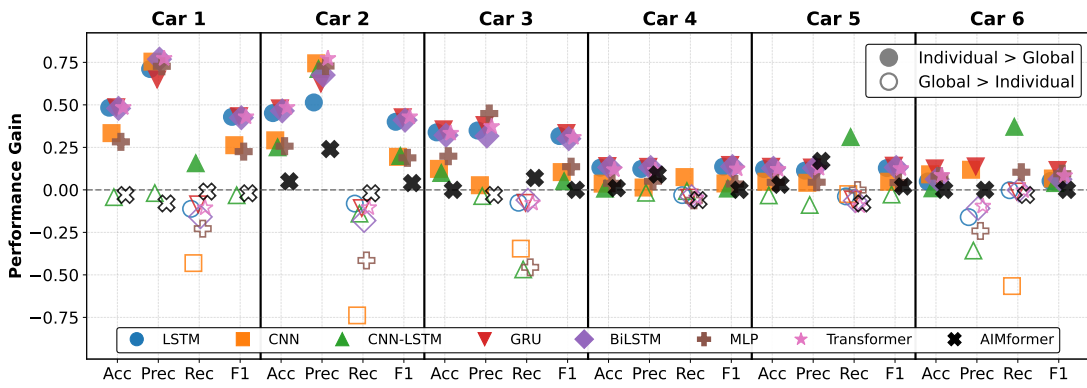
(a)



(b)



(c)



(d)

Fig. 4: PG controllers comparison. (a) Controller 1, (b) Controller 2, (c) Controller 3, (d) Controller 4.

erence absent accuracy degradation.

ONNX performs significantly worse: CPU-only inference requires $\approx 50\text{-}600\text{ms}$ (prohibitive for 10Hz CAM transmission); CUDA deployment reduces individual model latency to 10ms (viable but suboptimal). TensorRT achieves $0.75\text{-}0.8\text{ms}$ (global) and $\approx 0.4\text{ms}$ (individual), constituting a small fraction of single CAM intervals, enabling deployment on TensorRT-capable devices. TFLite exhibits the fastest quantized inference (0.13ms individual, 0.26ms global), requiring no additional hardware, making it ideal for both in-vehicle and RSU deployment.

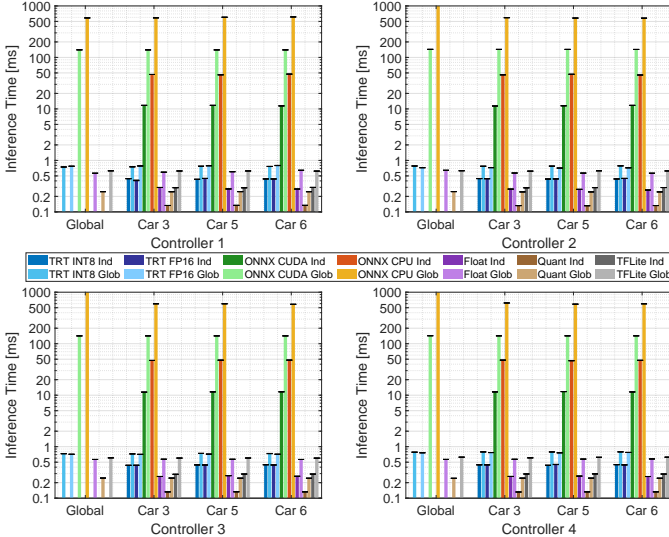


Fig. 5: Inference time comparison across quantization methods. Average latency (1000 runs) for global and individual models using TFLite, ONNX, and TensorRT with float16 and int8 quantization. Individual models infer 50-90% faster than global models, with TFLite int8 achieving optimal performance (0.13ms).

Fig. 6 compares TFLite and quantized model ROC curves. Both achieve high AUC with nearly identical curves, indicating quantization preserves accuracy. We analyze Cars 3, 5, and 6 (most impactful positions): Car 3 (immediate victim for all maneuvers) achieves high AUC with 0.1% difference between global and individual models; Car 5 (farthest from attacks, most challenging detection position) demonstrates high AUC despite difficulty, with global models superior for CVS controllers (1 and 2) but individual models superior for CTH controllers due to larger intra-platoon distances; Car 6 (joiner) performs similarly to Car 3, with both deployment approaches reliably detecting attacks. The worst performance occurs with the global model under Controller 1 due to divergent lane-change behavior, creating FPs, which highlights the limitations of universal global deployment.

Table VII compares model size. TFLite transformation reduces size by 50% (global) and 27% (individual); integer quantization achieves 86% (1.7 MB global) and 80% (1.2 MB individual) overall reduction. ONNX yields similar float quantization sizes (3.4 MB global, 2.3 MB individual) but larger integer sizes (3.3 MB global, 2 MB individual; 94% and 66% increases). TensorRT produces larger sizes (4.7 MB float

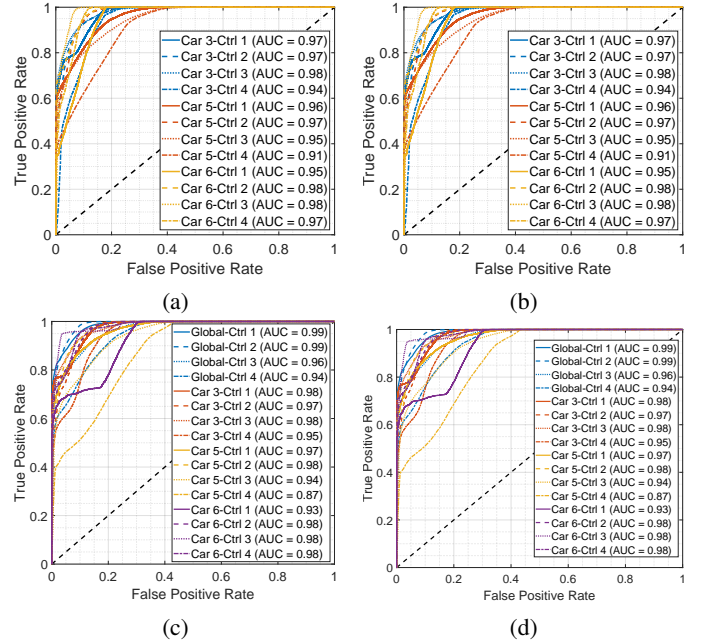


Fig. 6: ROC comparison for the TFLite and TFLite Quantized Individual and Global Models. (a) TFLite Individual, (b) Quant Individual, (c) TFLite Global, and (d) Quant Global.

TABLE VII: Model Sizes Comparison

Model	Model Size [MB]	
	Global	Individual
AIMFORMER	12.3	6.2
TFLite		
TFLite	6.6	4.5
Float	3.3	2.3
Dynamic Integer	1.7	1.2
ONNX		
Float	3.4	2.3
Integer	3.3	2
TensorRT		
Float	4.7	3
Integer	3	3

global, 3 MB float/integer individual), with 76-150% increases over TFLite, which also achieves the fastest inference.

Fig. 7 presents the energy consumption (Jetson 25W mode) for TFLite approaches. Global model differences are minimal ($2.66 \rightarrow 2.62\text{mJ}$ for Float, unchanged for Quant, $2.84 \rightarrow 2.79\text{mJ}$ for TFLite). Individual models achieve 46-52% energy reduction. Worst-case (TFLite global/global) requires ≈ 350 inferences per Watt (W).

D. Inter-Vehicle Aware Encoding

The previous sections demonstrated the superiority of the transformer-encoder in detecting misbehavior. Global models outperformed the individuals for vehicles downstream in the platoon, eliminating the need for multiple models. However, an extra step can be taken by changing Eq. 5 from $\mathbf{X}_{flat} = \text{reshape}(\mathbf{X}, [B \cdot V, T, F])$ to $\mathbf{X}_{flat} = \text{reshape}(\mathbf{X}, [B, V \cdot T, F])$. This reshaping captures spatio-temporal vehicle interactions through self-attention operating over the concatenated $V \cdot T$

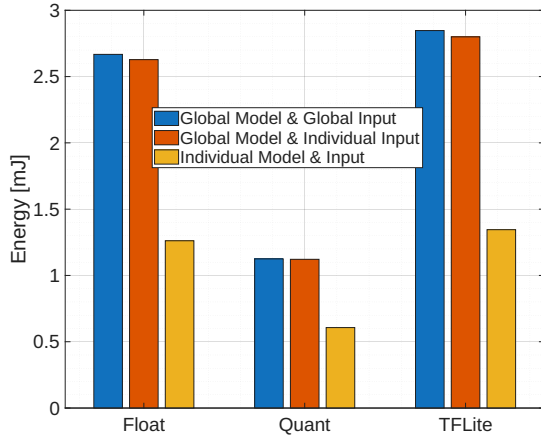


Fig. 7: Energy consumption for deployed models.

dimension, with global positional encoding providing temporal synchronization across the platoon. The unified attention mechanism models inter-vehicle coordination and intra-vehicle temporal dynamics jointly, requiring whole-platoon observations during both training and inference.

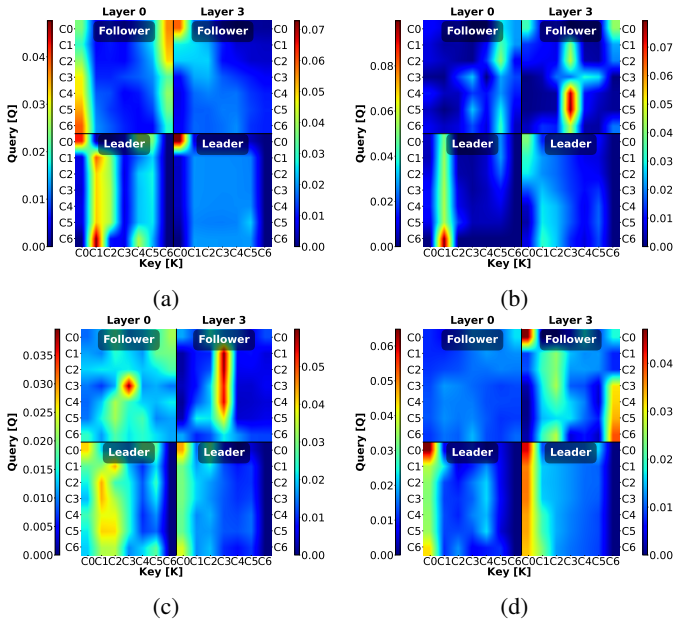


Fig. 8: Controllers comparison. (a) Controller 1, (b) Controller 2, (c) Controller 3, (d) Controller 4.

Fig. 8 presents the attention weights for layer 0 (input) and layer 3 (output) across all controllers in the case of attacks. Communication topology fundamentally shapes attention-based security strategies with distinct layer-wise progression and attack-adaptive patterns.

Controller 1 (PATH) employs leader and joiner monitoring for follower attacks ($C0-C6 \rightarrow C0, C6$ with gradient), while for leader attacks, Layer 0 shifts to victim monitoring ($C0-6 \rightarrow C1$) and Layer 3 maintains $C0$ -centric patterns, demonstrating attack-adaptive feature extraction with topology-invariant higher layers. Controller 2 (Ploeg), without leader visibility, progresses from minimal Layer 0 to focused Layer 3 back-

tracking ($C4-6 \rightarrow C3$) for follower attacks. For leader attacks, Layer 0 focuses on the victim ($C0$) while Layer 3 develops position-dependent stratification ($C0-2 \rightarrow C0, C3-6 \rightarrow C1$), compensating for topology constraints through distributed spatial detection. Controller 3 (Consensus) exhibits a “victim-versus-attacker” targeting strategy: follower attacks show $C3 \rightarrow C3$ self-monitoring (Layer 0) followed by collective validation $C0-6 \rightarrow C3$ (Layer 3). Meanwhile, the leader attacks unify the followers’ attention towards the victim, initially, the attacker, subsequently. Controller 4 (Flatbed) monitors multiple simultaneous targets for follower attacks: $C0 \rightarrow C0, C3-C5 \rightarrow C6$, as the joiner integrates behind attacker $C2$, while simultaneously focusing attention on attacker $V2$. For leader attacks, it presents a unified $C0-C6 \rightarrow C0$ attention across both layers.

Notably, this approach enables attack localization through the attention focus. For follower attacks, PATH monitors reference points ($C0, C6$) without specific attacker localization; Ploeg and Consensus attend to $V3$ (the immediate victim), enabling indirect localization through predecessor inference; while Flatbed achieves direct attacker ($C1-C4$ and $C6 \rightarrow C2$) and victim ($C3-C5 \rightarrow C6$) identification. For leader attacks, all controllers eventually scrutinize $C0$, facilitating direct source identification. These findings reveal a spectrum from leader monitoring (PATH) to victim-based inference (Ploeg, Consensus) to explicit source-targeting (Flatbed), with localization capability determined by whether attention focuses on attack symptoms, affected vehicles, or the attacker itself.

Fig. 9 presents the t-SNE visualizations of the controllers ($C1-C4$) with learned embeddings from the two transformer-encoder global architectures. The shaded regions are constructed using Kernel Density Estimation (KDE), showing the density regions of the data points. In both cases, we collect the same 2000 samples, allowing for a direct comparison of the clustering. Similar colors represent the classification of benign and attack data points for the same controller, while X colored notations correspond to FPs for that controller.

Fig. 9a showcases the inference result when the model processes each vehicle’s temporal sequences separately, whereas Fig. 9b illustrates the clustering based on the inter-vehicle attention. The former shows overlap between the benign/attack regions of $C1$ (blue regions), a high number of FPs for $C2$, and an overlap between $C2$ and $C4$. On the other hand, inter-vehicle attention (Fig. 9b) results in each controller occupying distinct regions, with clear separation between benign and attack regions, due to the capture of overall platoon behavioral patterns. There is a substantial decrease in the number of FPs for $C2$ with 3 FPs for $C3$.

To strengthen the argument for $V \cdot T$ ’s improvement, we present in Fig. 10 the comparison heatmap (similarly to Fig. 3). For global inference, $V \cdot T$ consistently outperformed $B \cdot V$, with F1-scores of 0.98, 0.98, 0.96, and 0.93 for controllers $C1-C4$, respectively, compared to $B \cdot V$ ’s 0.96, 0.96, 0.90, and 0.89. This advantage persists in individual vehicle inference (keeping in mind that $V \cdot T$ requires whole platoon input), where $V \cdot T$ maintains F1-scores above 0.90 for most vehicles while $B \cdot V$ exhibits greater variability (0.76-1.00). The performance gap is most evident in precision. $V \cdot T$ achieves near-perfect

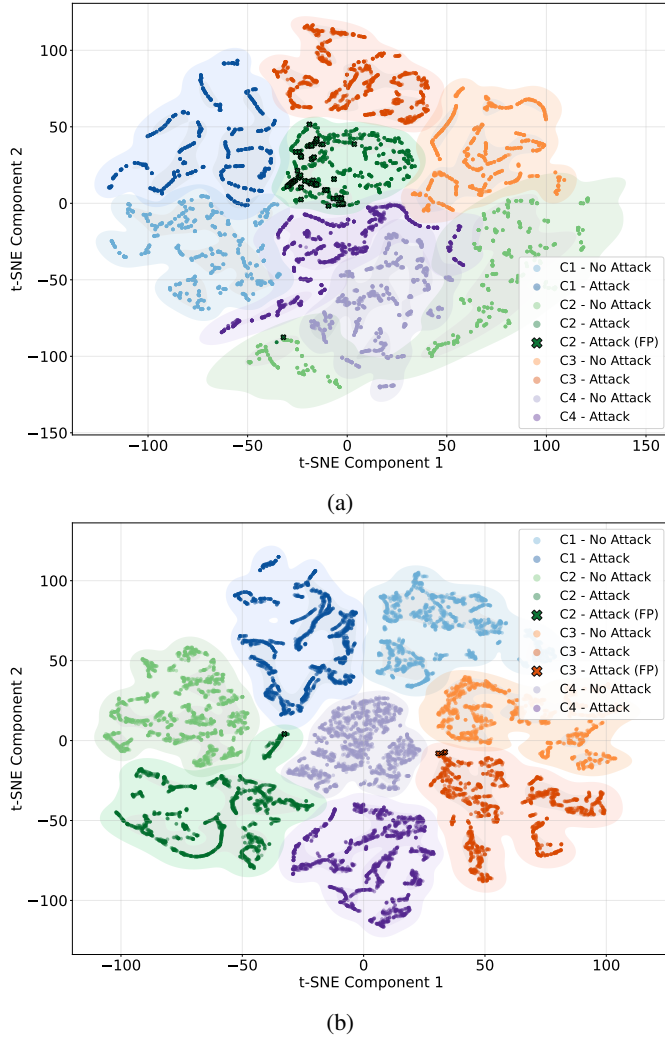


Fig. 9: t-SNE attention comparison: (a) Attending Time Windows vs. (b) Attending Vehicles.

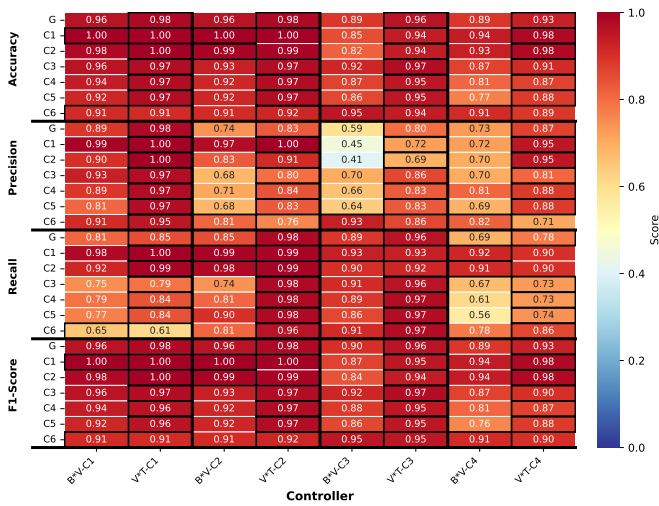


Fig. 10: Comparison between $B \cdot V$ and $V \cdot T$ global approaches.

precision (≥ 0.95) across controllers C1-C4, while $B \cdot V$ shows degradation for specific vehicles (0.41-0.59 for C1 and C2 under controller C3), suggesting that spatio-temporal attention effectively leverages cross-vehicle correlations to reduce false positives. $B \cdot V$ demonstrates competitive recall (0.91-0.93 for controller C3), indicating robust true positive detection despite lacking cross-vehicle context. The $V \cdot T$ architecture's unified attention over the $V \cdot T$ dimension captures synchronized multi-vehicle patterns, enabling it to leverage learned spatio-temporal priors even during single-vehicle inference. Conversely, $B \cdot V$ learns purely temporal patterns independently per vehicle, trading discriminative power for true vehicle-agnostic deployment capability. These results reveal a performance-flexibility trade-off. $V \cdot T$ offers superior accuracy (5-10% higher F1-scores) when complete platoon observations are available, while $B \cdot V$ maintains acceptable performance ($F1 \geq 0.87$ for almost all cases) with genuine vehicle independence, suitable for distributed deployment where vehicles perform local inference without inter-vehicle communication.

VI. DISCUSSION

Our comprehensive evaluation reveals distinct deployment strategies for various operational contexts, as well as limitations.

Vehicle-local deployment (individual models) suits upstream vehicles (positions 1-2) that exhibit position-specific patterns, privacy-constrained scenarios that limit platoon-wide data sharing, heterogeneous platoons with varying capabilities, and bandwidth-limited environments. The 50-90% inference speedup and 50% size reduction make individual models optimal for resource-constrained hardware. Nonetheless, a locally deployed $B \cdot V$ global model would enable the deployment of a single model, regardless of platoon position, at the cost of increased inference time (but still $< 1ms$) and memory footprint.

Infrastructure-based deployment (RSU-hosted $V \cdot T$ global models) maximizes detection performance, including attack localization, through platoon-wide input capturing cross-vehicle correlations. This approach is suitable for scenarios that require consistent platoon-wide performance and high-precision detection to minimize FPs.

Combining the two methods achieves an optimal balance: vehicles can deploy local models for low-latency detection, while querying RSU-hosted global models for more accurate detection and localization of the attacker, balancing accuracy, latency, communication overhead, and computational requirements.

Limitations and Future Directions. Our simulation-based evaluation could improve through real-world mobility testbed validation. The framework addresses known attack patterns (i.e., constant offset, gradual drift, and combined falsification); adaptive adversaries may craft evasion attacks, necessitating an investigation into adversarial robustness. Current deployment assumes static models; online learning and federated learning could enable privacy-preserving adaptation. While our PFBCE loss reduces FPs, comprehensive quantification of false alarm impacts on platoon operations remains unexplored. Finally,

extension to mixed autonomy scenarios with heterogeneous capabilities presents opportunities for future work, alongside integration with complementary security mechanisms, including cryptographic protocols and secure hardware.

VII. RELATED WORK

This section discusses misbehavior detection in VCs systems, transformer architectures for security applications, Deep Learning (DL) for vehicular security, and edge AI deployment.

A. Misbehavior Detection in Vehicular Networks

Misbehavior detection in IoV environments has evolved from rule-based plausibility checks to ML-based approaches. Van der Heijden et al. [61] provided a comprehensive survey identifying fundamental challenges in cooperative ITS, including the difficulty of distinguishing between benign sensor errors and malicious data falsification. Boualouache and Engel [39] extended this analysis to 5G-enabled vehicular networks, emphasizing the need for real-time detection capabilities that scale with increasing network density.

Frameworks have been essential for advancing the field. Kamel et al. [41] introduced the VeReMi dataset, providing the first reproducible benchmark for comparing misbehavior detection algorithms across diverse attack scenarios. The VeReMi Extension [62] expanded coverage to include additional attack vectors and environmental conditions, becoming the de facto standard for evaluating detection approaches. So et al. [45] demonstrated that combining Physical (PHY)-layer plausibility checks with traditional position verification improves detection rates by 15-20%, achieving 83-95% accuracy against falsification attacks.

ML integration has shown substantial promise. Sharma and Liu [63] developed a data-centric model achieving 94% detection accuracy by leveraging ensemble methods, while Gyawali et al. [49] incorporated reputation techniques to reduce FP rates in dynamic network topologies. Privacy-preserving approaches have gained attention, with Upreti et al. [51] proposing Federated Learning (FL) for distributed misbehavior detection that maintains 92% accuracy while preserving location privacy.

Platoon-specific security research remains limited. Previous work [7] characterized attack impact across different platoon controllers and topologies, revealing that acceleration falsification poses the greatest threat to string stability. However, existing detection mechanisms struggle with combined attacks that manipulate multiple kinematic parameters in physically consistent patterns—a gap our transformer-based approach addresses.

B. Transformers for Security and Anomaly Detection

Transformer architectures revolutionized sequence modeling tasks, with recent applications for cybersecurity. Xu et al. [64] introduced *Anomaly Transformer*, leveraging association discrepancy to identify temporal anomalies in multivariate time series with 98.2% AUC on benchmark datasets. Tuli et al. [65] proposed *TranAD*, demonstrating that deep transformer

networks outperform LSTM-based approaches by 8-12% for multivariate time series anomaly detection through parallel processing of temporal dependencies.

Self-supervised learning has enhanced the effectiveness of transformers for security tasks. Jeong et al. [66] developed *AnomalyBERT*, which employs data degradation schemes during pre-training to achieve robust anomaly detection without extensive labeled data, particularly relevant for vehicular environments where attack samples are scarce. Long et al. [67] applied transformers to cloud network intrusion detection, achieving 97.3% accuracy with significantly reduced false positive rates compared to traditional DNN approaches.

Despite these advances, transformer applications for vehicular misbehavior detection remained unexplored. Existing work focuses on network traffic analysis or generic time series anomaly detection, lacking the domain-specific considerations necessary for understanding the dynamics of platoon coordination. Our AIMFORMER architecture addresses this gap through global positional encoding mechanisms that capture cross-vehicle temporal relationships and custom loss functions optimized for the requirements of safety-critical vehicular applications.

C. Deep Learning for Vehicular Security

DL approaches have become predominant in vehicular security research, with LSTM and CNN architectures achieving substantial detection performance. For misbehavior detection in VANET environments, Alladi et al. [44] developed a DL-based classification scheme achieving 95.7% accuracy across nine attack categories in cooperative ITS. Hsieh et al. [46] proposed an integrated CNN-LSTM architecture that captures both spatial feature patterns and temporal dependencies, demonstrating 93.2% detection rates on the VeReMi dataset.

In-vehicle network security has received considerable attention. Kang and Kang [50] applied DNN for CAN bus intrusion detection, achieving 99.7% accuracy for binary classification tasks. Song et al. [52] extended this work with convolutional architectures that automatically extract message timing patterns, while Longari et al. [54] employed LSTM autoencoders for unsupervised anomaly detection with 99.2% AUC. Javed et al. [56] combined CNN with attention-based GRU to achieve state-of-the-art performance (99.5% accuracy) for controller area network intrusion detection.

Hybrid architectures have shown promise for complex vehicular scenarios. Sun et al. [58] proposed a CNN-LSTM with attention for spatiotemporal feature extraction, demonstrating improved detection of multi-stage attacks. Zhu et al. [59] investigated mobile edge-assisted deployment of LSTM models, achieving real-time inference ($< 50ms$ latency) on resource-constrained edge servers.

FL approaches address privacy concerns in distributed vehicular networks. Gurjar et al. [48] proposed a FL-based misbehavior classification framework achieving 98.6% accuracy while preserving vehicle location privacy. However, these approaches typically require substantial computational resources for model training and aggregation, which limits their practical deployment on edge platforms.

TABLE VIII: Comparison of Misbehavior Detection in Vehicular Networks. Column Deploy: ○ = Not appropriate HW (not OBU/Edge); ● = Appropriate HW (OBU/Edge); ● = HW + Quantization. Metrics: A=Accuracy; P=Precision; R=Recall

Ref.	Platoon	Architecture	Deploy	Inference Time [ms]	Metrics [%]	Attacks	Controller	Ref.	Platoon	Architecture	Deploy	Inference Time [ms]	Metrics	Attacks	Controller
[41]	No	Plausibility	○	✗	P:40-99, R:40-99	Pos/Speed falsif.	N/A	[42]	No	3/4/5x LSTM, CNN-LSTM	○	✗	A:98, P:97, R:99	Pos/spd. falsif.	N/A
[43]	No	Plaus. + cons., MLP	○	–	Det:✓	Stale msg., falsif.	–	[44]	No	CNN-LSTM, GRU, AE	○	–	A:98, P:97, R:96	Pos/spd. falsif.	–
[45]	No	RSSI vs. k-NN/SVM	●	–	A:87-94, P:87-99, R:61-84	Pos. falsif.	–	[46]	No	CNN-LSTM-SVM	○	–	A:95.4, F1:96.1	Pos. falsif.	–
[47]	No	Ens. (RF, SVM, k-NN)	○	–	A:81-92, P:82-95, R:79-90, F1:✓	Pos. falsif.	–	[48]	No	FedAvg, FedProx	○	–	A:93, P:92, R:91, F1:92	19 VeReMi types	–
[49]	No	RF + Dempster-Shafer	○	2.0	P:86-99, R:46-99, F1:89-96	Sybil, DoS	–	[50]	No	DNN with DBN	○	2-5	A:99.7, P:99, R:99, AUC:99	Pkt. inj., manip.	–
[51]	No	FedML (SVM, LSTM)	○	–	A:92, P:93, R:90	Pos. falsif.	–	[52]	No	Deep CNN (Inc-ResNet)	●	5-7	A:99.99, P:99, R:99	DoS, spoofing	–
[53]	No	DNN w/ seq. recon.	○	–	Anom:✓, Gain:✓	Pos./spd. falsif.	–	[54]	No	LSTM Autoencoder	●	650	AUC:0.97, F1:0.95	Replay, manip.	–
[55]	No	k-NN, RF, Ensemble	○	–	P:94-98, R:85-93, F1:89-96	Pos. falsif., DoS	–	[56]	No	CNN + Attn-GRU	○	–	A:99, Gain:10.8%	Mixed intrusion	–
[57]	No	DBN, LSTM, GRU, RF	○	0.05-1.16	A:75-92 (2-step)	Pos. falsif.	–	[58]	No	CNN-LSTM + Attn	○	–	F1:0.95, ER:2.16%, A:97.8	Multi-attack CAN	–
[59]	No	Multi-task LSTM	●	0.61-144	A:90, P:89, R:88	Multi-dim. anom.	–	[60]	Part.	GMM-MDN w/ RNN	○	–	Cons:✓, Det:✓	Vel., acc. falsif.	–
[7]	Yes	GMM-HMM	○	130-280	F1:87, P:88, R:86	Pos./spd./acc., jam	SUMO CACC	[16]	Yes	RF	○	10	Coll:58→2%, Det:✓	Pos. mutation	Santini
[19]	Part.	LSTM/GRU	○	–	Stealth:✓, Det:✓	Stealth attacks	ACC/CACC	[20]	Yes	LSTM	○	–	A:96, Det:✓	Corr./non-corr.	CACC
[17]	Part.	MLP	●	–	Det:✓, Resil:✓	Comm. DoS	CACC	[18]	Yes	Set-membership	○	–	Stab:✓, Det:✓	DoS, deception	Leader-fol.
Ours	Yes	Transformer (MHA)	●	0.13-0.8	A:✓, P:✓, R:✓, F1:✓, AUC:96-99, ROC:✓	Pos./spd./acc. (stealth)	SUMO CACC	[5]	Yes	Transformer (MHA)	○	100-500	A:88-92, P:91-93, R:88-92, F1:89-92, AUC:96-99	Pos./spd./acc. (stealth)	Multiple CACC

While achieving high accuracy, existing DL approaches face limitations: LSTM architectures struggle with long-range temporal dependencies essential for analyzing platoon coordination, and CNN-based methods require careful manual feature engineering for time series data. Furthermore, most prior work evaluates detection performance in isolation rather than considering an end-to-end pipeline from data collection to edge deployment.

D. Edge AI for Vehicular and IoT Networks

Edge AI has emerged as an enabling technology for real-time vehicular security, addressing latency and privacy constraints inherent in cloud-centric approaches. Gong et al. [68] identify three key deployment paradigms: on-vehicle inference, roadside unit processing, and hybrid edge-cloud architectures. Zhang and Letaief [23] demonstrated that edge intelligence can reduce end-to-end latency by 10-15x compared to cloud processing while maintaining comparable accuracy; essential for safety-critical vehicular applications with sub-100ms response requirements.

Tiny Machine Learning (TinyML) frameworks enable deployment on resource-constrained hardware. De Prado et al. [69] demonstrated deployment of DNN models on autonomous mini-vehicles using model quantization, achieving 3-5x energy efficiency improvements with minimal accuracy degradation (< 2%). Alajlan and Ibrahim [70] provided a comprehensive overview of TinyML techniques for Internet of Things (IoT) edge devices, emphasizing the importance of model architecture and target hardware co-design.

DNN inference acceleration in vehicular edge computing has received substantial research attention. Liu et al. [71] proposed joint optimization of task partitioning and edge resource allocation, achieving 40% latency reduction with 99% reliability guarantees for safety-critical inference tasks. Li et al. [72] developed mobility-aware acceleration strategies that adapt model partitioning based on vehicle trajectory predictions, maintaining inference quality during handover events.

FL approaches balance privacy preservation with model performance in distributed vehicular environments. Valente et al. [73] demonstrated embedded FL for VANET environments, achieving 94.3% accuracy with on-vehicle training on Raspberry Pi-class hardware. Mughal et al. [74] proposed adaptive FL with multi-edge clustering, reducing communication overhead by 60% while maintaining convergence properties. Pervej et al. [75] addressed highly mobile scenarios, developing a resource-constrained vehicular edge FL that maintains 93% accuracy despite frequent topology changes.

Model quantization techniques enable the deployment of AI on edge platforms [27]. Recent work [28], [29] has demonstrated that 8-bit integer quantization can reduce transformer model sizes by 4x with < 1% accuracy degradation for classification tasks. However, the impact of quantization on transformer-based misbehavior detection for vehicular platoons remains unexplored, particularly regarding the precision-recall trade-offs critical for safety-critical applications.

E. Positioning of Our Work

Table VIII compares AIMFORMER with existing frameworks. Our work builds upon foundational contributions in vehicular misbehavior detection, particularly VeReMi [41] for plausibility-based validation, and extends recent advances in ensemble methods [47], [55], FL [51], [48], and recurrent architectures [42], [44], [46]. While these approaches demonstrate strong detection capabilities in general VANET contexts, they face limitations when applied to the strict real-time requirements and dynamic operational characteristics of platoon systems.

Within platoon-focused detection, prior approaches span probabilistic methods (GMM-HMM, 87% F1, 130-280ms) [7], recurrent networks (LSTM/GRU, > 96% accuracy) [19], [20], and specialized methods (RF, 10ms inference) [16], [17], [18]. Most directly, our work builds on AttentionGuard [5], which achieves 88-92% accuracy and 96-99% AUC but with inference times of 100-500ms, precluding practical edge deployment.

AIMFORMER advances beyond AttentionGuard and the broader landscape through four key contributions: (1) integrated quantization-aware training achieving the first transformer-based detector with sub-millisecond inference (0.13-0.8ms versus 100-500ms), enabling practical On-Board Unit (OBU)/edge deployment; (2) unified framework handling position, speed, and acceleration falsification including stealth variants through adaptive masking and global positional encoding, whereas prior work targets specific attack types [16] or scenarios [19]; (3) two to three orders of magnitude faster inference while maintaining superior detection performance (96-99% AUC); (4) comprehensive evaluation including different maneuvers (i.e., join, exit, lane change) representing critical vulnerability windows that prior work does not systematically address [5], [7], [20].

To summarize, AIMFORMER delivers a complete solution combining high detection accuracy with practical edge deployment feasibility, addressing the fundamental challenge of deploying DL models on resource-constrained vehicular hardware while advancing beyond probabilistic [7], recurrent [19], [20], specialized [16], and our prior transformer-based work [5].

VIII. CONCLUSION

We presented AIMFORMER, a transformer-based framework for misbehavior detection tailored specifically to vehicular platooning environments. Our framework incorporates domain-specific techniques, including global positioning encoding with temporal offsets, as well as a precision-focused loss function. These components effectively address the unique challenges of detecting malicious behavior in coordinated multi-vehicle systems. AIMFORMER simultaneously models inter-vehicle temporal dependencies and spatial correlations, enabling robust detection across heterogeneous control strategies and attack vectors while maintaining the computational efficiency required for safety-critical applications. Our comprehensive evaluation establishes AIMFORMER's superiority over existing DNN architectures, demonstrating consistent performance gains across various attack scenarios with an AUC of 96-99%. Moreover, deployment analysis validates the practical feasibility of sub-millisecond inference latencies, achievable through model quantization and optimization, enabling both vehicle-local and infrastructure-based deployments.

REFERENCES

- [1] P. Papadimitratos *et al.*, "Secure Vehicular Communication Systems: Design and Architecture," *IEEE Comm. Mag.*, Nov. 2008.
- [2] Amoozadeh *et al.*, "Platoon management with cooperative adaptive cruise control enabled by vanet," *Vehicular Communications*, 2015. [Online]. Available: <https://www.sciencedirect.com/science/article/pii/S2214209615000145>
- [3] —, "Security Vulnerabilities of Connected Vehicle Streams and Their Impact on Cooperative Driving," *IEEE Comm. Mag.*, Jun. 2015.
- [4] K. Kalogiannis, M. Hartmann, and P. Papadimitratos, "Prime: Platoon restructuring for incident mitigation and exclusion," in *International Conference on Wireless and Mobile Computing, Networking and Communications (WiMob)*, 2024.
- [5] H. Li, K. Kalogiannis, A. M. Hussain, and P. Papadimitratos, "AttentionGuard: Transformer-based Misbehavior Detection for Secure Vehicular Platoons," in *ACM Workshop on Wireless Security and Machine Learning (WiseML)*, 2025.
- [6] M. A. Abdelmaguid, H. S. Hassanein, and M. Zulkernine, "Beyond the Attack: Strategies for Attack Endgame Mitigation in VANETS," *IEEE TVT*, 2025.
- [7] K. Kalogiannis, M. Khodaei, W. M. N. M. Bayaa, and P. Papadimitratos, "Attack impact and misbehavior detection in vehicular platoons," in *Proceedings of the 15th ACM Conference on Security and Privacy in Wireless and Mobile Networks*, 2022.
- [8] Heijden *et al.*, "Analyzing Attacks on Cooperative Adaptive Cruise Control (CACC)," in *IEEE VNC*, Torino, Italy, Nov. 2017.
- [9] Calandriello *et al.*, "On the Performance of Secure Vehicular Communication Systems," *IEEE TDSC*, November 2011.
- [10] M. Khodaei *et al.*, "SECMACE: Scalable and Robust Identity and Credential Management Infrastructure in Vehicular Communication Systems," *IEEE T-ITS*, May 2018.
- [11] M. Khodaei and P. Papadimitratos, "Scalable & Resilient Vehicle-Centric Certificate Revocation List Distribution in Vehicular Communication Systems," *IEEE TMC*, 2021.
- [12] Grover *et al.*, "Machine learning approach for multiple misbehavior detection in vanet," in *International conference on advances in computing and communications*. Springer, 2011.
- [13] S. A. Abdel Hakeem and H. Kim, "Advancing Intrusion Detection in V2X Networks: A Comprehensive Survey on Machine Learning, Federated Learning, and Edge AI for V2X Security," *IEEE T-ITS*, 2025.
- [14] K. Kalogiannis, "Investigating attacks on vehicular platooning and cooperative adaptive cruise control," 2020.
- [15] K. Kalogiannis, A. Henriksson, and P. Papadimitratos, "Vulnerability analysis of vehicular coordinated maneuvers," in *IEEE EuroS&PW*, 2023.
- [16] Boddupalli *et al.*, "Replace: Real-time security assurance in vehicular platoons against v2v attacks," in *IEEE ITSC*, 2021.
- [17] S. Boddupalli and S. Ray, "Redem: Real-time detection and mitigation of communication attacks in connected autonomous vehicle applications," in *IFIP international Internet of Things conference*. Springer, 2019.
- [18] E. Mousavinejad and L. Vlacic, "Secure platooning control of automated vehicles under cyber attacks," *ISA transactions*, 2022.
- [19] Wang *et al.*, "Deep-learning-based intrusion detection for autonomous vehicle-following systems," in *IEEE ITSC*, 2021.
- [20] B. Ko and S. H. Son, "An approach to detecting malicious information attacks for platoon safety," *IEEE Access*, 2021.
- [21] Vaswani *et al.*, "Attention is all you need," *Advances in neural information processing systems*, 2017.
- [22] Lin *et al.*, "The architectural implications of autonomous driving: Constraints and acceleration," ser. ASPLOS '18. New York, NY, USA: Association for Computing Machinery, 2018. [Online]. Available: <https://doi.org/10.1145/3173162.3173191>
- [23] J. Zhang and K. B. Letaief, "Mobile edge intelligence and computing for the Internet of Vehicles," *Proceedings of the IEEE*, 2020.
- [24] C. Hendrix and G. Bloom, "Platoon vulnerability due to network topology and targeted vehicle," in *IEEE CCNC*, 2024.
- [25] Filho *et al.*, "A systematic literature review on distributed machine learning in edge computing," *Sensors*, 2022.
- [26] Murshed *et al.*, "Machine learning at the network edge: A survey," *ACM Comput. Surv.*, Oct. 2021. [Online]. Available: <https://doi.org/10.1145/3469029>
- [27] A. Hussain, N. Abughanam, J. Qadir, and A. Mohamed, "Jamming Detection in IoT Wireless Networks: An Edge-AI based Approach," in *Proceedings of the 12th International Conference on the Internet of Things (IoT)*, 2022.
- [28] A. M. Hussain, N. Abughanam, and P. Papadimitratos, "Edge AI-based Radio Frequency Fingerprinting for IoT Networks," *arXiv preprint arXiv:2412.10553*, 2024.
- [29] A. Hussain, N. Abughanam, and P. Papadimitratos, "Towards a Lightweight Edge AI-based Radio Frequency Fingerprinting," in *International Wireless Communications and Mobile Computing (IWCMC)*, Abu Dhabi, United Arab Emirates, May 2025.
- [30] Papadimitratos *et al.*, "Vehicular Communication Systems: Enabling Technologies, Applications, and Future Outlook on Intelligent Transportation," *IEEE Communications Magazine*, November 2009.
- [31] "Ieee standard for wireless access in vehicular environments—security services for application and management messages," *IEEE Std 1609.2-2022 (Revision of IEEE Std 1609.2-2016)*, 2023.
- [32] M. Khodaei, H. Noroozi, and P. Papadimitratos, "Secmace+: Upscaling pseudonymous authentication for large mobile systems," *IEEE TCC*, 2023.
- [33] P. Papadimitratos, V. Gligor, and J.-P. Hubaux, "Securing Vehicular Communications-Assumptions, Requirements, and Principles," in *Workshop on Embedded Security in Cars (ESCAR)*, November 2006.

- [34] Y. G. Dantas, V. Nigam, and C. Talcott, "A Formal Security Assessment Framework for Cooperative Adaptive Cruise Control," in *IEEE VNC*, NY, USA, Dec. 2020.
- [35] S. Ucar *et al.*, "IEEE 802.11 p and Visible Light Hybrid Communication Based Secure Autonomous Platoon," *IEEE TVT*, May 2018.
- [36] Li *et al.*, "Hyperband: A novel bandit-based approach to hyperparameter optimization," *Journal of Machine Learning Research*, 2018.
- [37] C. S. Han, H. Kim, and K. M. Lee, "Reevaluating the potential of a vanilla transformer encoder for unsupervised time series anomaly detection in sensor applications," *Sensors*, 2025.
- [38] Restack, "Hyperparameter tuning for transformer models [online]," <https://www.restack.io/p/hyperparameter-tuning-answer-transformer-models-cat-ai>, 2024.
- [39] A. Boualouache and T. Engel, "A survey on machine learning-based misbehavior detection systems for 5g and beyond vehicular networks," *IEEE Communications Surveys & Tutorials*, 2023.
- [40] Almeshdar *et al.*, "Deep learning in the fast lane: A survey on advanced intrusion detection systems for intelligent vehicle networks," *IEEE Open Journal of Vehicular Technology*, 2024.
- [41] Heijden *et al.*, "Veremi: A dataset for comparable evaluation of misbehavior detection in vanets," in *14th International Conference, SecureComm 2018, Singapore, Singapore, August 8-10, 2018*, 2018.
- [42] Alladi *et al.*, "Securing the internet of vehicles: A deep learning-based classification framework," *IEEE Networking Letters*, 2021.
- [43] Kamel *et al.*, "Simulation framework for misbehavior detection in vehicular networks," *IEEE TVT*, 2020.
- [44] T. Alladi, V. Kohli, V. Chamola, and F. R. Yu, "A deep learning based misbehavior classification scheme for intrusion detection in cooperative intelligent transportation systems," *Digital Communications and Networks*, 2023.
- [45] S. So, J. Petit, and D. Starobinski, "Physical layer plausibility checks for misbehavior detection in V2X networks," in *Proceedings of the 12th Conference on Security and Privacy in Wireless and Mobile Networks*, ser. WiSec '19. ACM, 2019.
- [46] C.-Y. Hsieh, Y.-L. Hsu, and J.-W. Perng, "A deep learning-based integrated algorithm for misbehavior detection system in VANETS," in *Proceedings of the ACM International Conference on Intelligent Computing and its Emerging Applications*, ser. ICAISE. ACM, 2021.
- [47] S. Ercan, M. Ayaida, and N. Messai, "Misbehavior Detection for Position Falsification Attacks in VANETS Using Machine Learning," *IEEE Access*, 2022.
- [48] D. Gurjar, J. Grover, V. Kheterpal *et al.*, "Federated learning-based misbehavior classification system for VANET intrusion detection," *Journal of Intelligent Information Systems*, 2025.
- [49] S. Gyawali, Y. Qian, and R. Q. Hu, "Machine learning and reputation based misbehavior detection in vehicular communication networks," *IEEE TVT*, 2020.
- [50] M.-J. Kang and J.-W. Kang, "Intrusion detection system using deep neural network for in-vehicle network security," *PLOS ONE*, 2016.
- [51] A. Uprety, D. B. Rawat, and J. Li, "Privacy preserving misbehavior detection in IoV using federated machine learning," in *IEEE 18th Annual Consumer Communications & Networking Conference (CCNC)*, 2021.
- [52] H. M. Song, J. Woo, and H. K. Kim, "In-vehicle network intrusion detection using deep convolutional neural network," *Vehicular Communications*, 2020.
- [53] Alladi *et al.*, "Deep neural networks for securing iot enabled vehicular ad-hoc networks," in *IEEE ICC*, 2021.
- [54] Longari *et al.*, "CANnolo: An anomaly detection system based on LSTM autoencoders for controller area network," *IEEE Transactions on Network and Service Management*, 2021.
- [55] S. Gyawali and Y. Qian, "Misbehavior Detection using Machine Learning in Vehicular Communication Networks," in *IEEE ICC*, 2019.
- [56] Javed *et al.*, "CANintelliIDS: Detecting in-vehicle intrusion attacks on a controller area network using CNN and attention-based GRU," *IEEE TNSE*, 2021.
- [57] N. C. Kushardianto, Y. E. Hillali, and C. Tatkeu, "2-step prediction for detecting attacker in vehicle to vehicle communication," in *IEEE VTC*, 2021.
- [58] Sun *et al.*, "Anomaly detection for in-vehicle network using CNN-LSTM with attention mechanism," *IEEE TVT*, 2021.
- [59] Zhu *et al.*, "Mobile edge assisted literal multi-dimensional anomaly detection of in-vehicle network using LSTM," *IEEE TVT*, 2019.
- [60] A. Sarker and H. Shen, "A data-driven misbehavior detection system for connected autonomous vehicles," *Proc. ACM Interact. Mob. Wearable Ubiquitous Technol.*, Dec. 2018. [Online]. Available: <https://doi.org/10.1145/3287065>
- [61] Heijden *et al.*, "Survey on misbehavior detection in cooperative intelligent transportation systems," *IEEE Communications Surveys & Tutorials*, 2019.
- [62] Kamel *et al.*, "VeReMi extension: A dataset for comparable evaluation of misbehavior detection in VANETS," in *IEEE ICC*, 2020.
- [63] P. Sharma and H. Liu, "A machine-learning-based data-centric misbehavior detection model for Internet of Vehicles," *IEEE IoT-J*, 2021.
- [64] J. Xu, H. Wu, J. Wang, and M. Long, "Anomaly transformer: Time series anomaly detection with association discrepancy," in *International Conference on Learning Representations (ICLR)*, 2022, arXiv:2110.02642.
- [65] S. Tuli, G. Casale, and N. R. Jennings, "TranAD: Deep transformer networks for anomaly detection in multivariate time series data," *Proceedings of the VLDB Endowment*, 2022, arXiv:2201.07284.
- [66] Jeong *et al.*, "AnomalyBERT: Self-supervised transformer for time series anomaly detection using data degradation scheme," *arXiv preprint arXiv:2305.04468*, 2023.
- [67] Long *et al.*, "A transformer-based network intrusion detection approach for cloud security," *Journal of Cloud Computing*, 2024.
- [68] T. Gong, L. Zhu, F. R. Yu, and T. Tang, "Edge intelligence in intelligent transportation systems: A survey," *IEEE Transactions on Intelligent Transportation Systems*, 2023.
- [69] de Prado *et al.*, "Robustifying the deployment of tinyML models for autonomous mini-vehicles," *Sensors*, 2021.
- [70] N. N. Alajlan and D. M. Ibrahim, "TinyML: Enabling of inference deep learning models on ultra-low-power IoT edge devices for AI applications," *Micromachines*, 2022.
- [71] Liu *et al.*, "Accelerating DNN inference with reliability guarantee in vehicular edge computing," *IEEE/ACM Transactions on Networking*, 2023.
- [72] Li *et al.*, "DNN inference acceleration based on adaptive task partitioning and offloading in embedded VEC," *ACM Transactions on Embedded Computing Systems*, 2025.
- [73] Valente *et al.*, "Embedded federated learning for VANET environments," *Applied Sciences*, 2023.
- [74] Mughal *et al.*, "Adaptive federated learning for resource-constrained IoT devices through edge intelligence and multi-edge clustering," *Scientific Reports*, 2024.
- [75] M. F. Pervej, R. Jin, and H. Dai, "Resource constrained vehicular edge federated learning with highly mobile connected vehicles," *IEEE Journal on Selected Areas in Communications*, 2023.

Konstantinos Kalogiannis is a PhD Candidate in the Networked Systems Security (NSS) Group at KTH Royal Institute of Technology, Stockholm, Sweden, where he also received his M.Sc. degree. Prior to his doctoral studies, he worked as a researcher in the NSS Group at KTH. His research interests include security and privacy in cyber-physical systems, with a focus on vehicular ad hoc networks (VANETS) and platooning, as well as cloud infrastructure deployment and services, and the security analysis of large-scale software systems. He has served as a reviewer for IEEE Communications Letters, IEEE Transactions on Intelligent Transportation Systems, IEEE Transactions on Vehicular Technology, and IEEE Open Journal of Vehicular Technology.

Ahmed Mohamed Hussain is currently a Pre-Doctoral Researcher with the Networked Systems Security (NSS) Group at KTH Royal Institute of Technology, Sweden. Prior to joining KTH, he was a researcher with the Computer Science and Engineering department at Qatar University, Doha, Qatar. He holds a Master's degree in Computer Science from Uppsala University, Sweden. Ahmed has received recognition for his research contributions, including the IWCMC 2024 Best Paper Award and WiMob 2025 Best Paper Award Runner-Up. He serves regularly as a reviewer for multiple journals, including IEEE TRANSACTIONS and various conferences. His research interests encompass IoT security and privacy, wireless network security, physical layer security, and the application of artificial intelligence to cybersecurity challenges.

Hexu Li is currently a Researcher working with the Tech Validation – AI department at the Chief Technology Officer (CTO) Organization, Lenovo, Beijing, China. He received his Master's degree in Communication Systems from the KTH Royal Institute of Technology, Stockholm, Sweden, where he conducted his thesis research at the Networked Systems Security (NSS) Group. He also holds a Bachelor's degree in Communication Engineering from Dalian Maritime University, China.

Panos Papadimitratos earned his Ph.D. degree from Cornell University, Ithaca, NY, USA. He leads the Networked Systems Security group at KTH, Stockholm, Sweden. He serves as a member (and currently chair) of the ACM WiSec conference steering committee, member of the PETS Advisory Board, and the CANS conference steering committee. Panos is an IEEE Fellow, a Young Academy of Europe Fellow, a Knut and Alice Wallenberg Academy Fellow, and an ACM Distinguished Member. His group webpage is: www.eecs.kth.se/nss.